

See discussions, stats, and author profiles for this publication at: <https://www.researchgate.net/publication/10848172>

# Structural and Functional Properties of *Yersinia pestis* Caf1 Capsular Antigen and Their Possible Role in Fulminant Development of Primary Pneumonic Plague

ARTICLE in JOURNAL OF PROTEOME RESEARCH · APRIL 2002

Impact Factor: 4.25 · DOI: 10.1021/pr025511u · Source: PubMed

---

CITATIONS

9

---

READS

54

11 AUTHORS, INCLUDING:



Vladimir N Uversky

University of South Florida

656 PUBLICATIONS 33,873 CITATIONS

SEE PROFILE

## Structural and Functional Properties of *Yersinia pestis* Caf1 Capsular Antigen and Their Possible Role in Fulminant Development of Primary Pneumonic Plague

Vyacheslav M. Abramov,<sup>†</sup> Anatoly M. Vasiliev,<sup>†</sup> Valentin S. Khlebnikov,<sup>†</sup> Raisa N. Vasilenko,<sup>†</sup> Nataly L. Kulikova,<sup>†</sup> Igor V. Kosarev,<sup>†</sup> Alexander T. Ishchenko,<sup>†</sup> Joel R. Gillespie,<sup>‡</sup> Ian S. Millett,<sup>§</sup> Anthony L. Fink,<sup>‡</sup> and Vladimir N. Uversky<sup>\*,†,‡,||</sup>

Institute of Immunological Engineering, 142380 Lyubuchany, Moscow Region, Russia, Department of Chemistry and Biochemistry, University of California, Santa Cruz, California 95064, Departments of Physics and Chemistry, Stanford University, Stanford, California 94305, and Institute for Biological Instrumentation, Russian Academy of Sciences, 142292 Pushchino, Moscow Region, Russia

Received February 8, 2002

*Yersinia pestis* capsular antigen Caf1 is shown to be a  $\beta$ -structural protein that in polymeric form possesses very high conformational stability. Different approaches show that a dimer is the minimal cooperative block of Caf1 adhesin. Caf1 dimer interacts effectively with IL-1 receptors of human macrophage and epithelial cells. The specificity of such interaction is confirmed by the inhibition of IL-1 $\alpha$  binding by Caf1. The Caf1 role in pneumonic plague pathogenesis is discussed.

**Keywords:** bubonic plague • pneumonic plague • capsular antigen Caf1 • molecular adhesin • conformational stability

### Introduction

Since Biblical times, mankind has suffered from the worldwide manifestation of the plague pandemics. "The effect of this natural and human disaster changed Europe profoundly, perhaps more so than any other series of events. For this reason, alone, the Black Death should be ranked as the greatest biological-environmental event in history, and one of the major turning points of Western Civilization".<sup>1</sup> *Yersinia pestis*, the causative agent of human bubonic and pneumonic plague, has killed more people than all wars during human history. It has been estimated that 200 million people may have died from plague, which is still active in various regions of the world.<sup>2–5</sup> In the past decade, the situation has worsened with the reemergence of plague in areas where it was absent for several years, including India, Madagascar, and Mozambique.<sup>5</sup> Recently, a serious new threat has appeared—the possible use of *Y. pestis* as a weapon in the hands of bioterrorists.<sup>6,7</sup>

Primary pneumonic plague is the most dangerous epidemiologically and the most severe infection.<sup>4</sup> Development of the infectious process is determined by the entry for *Y. pestis* bacteria, to which skin and mucous membranes form only a weak barrier. The beginning of the disease is sudden, without a prodromal period, with temperature elevation to 39–40 °C and death usually by the second to fourth day. Despite much effort, the mechanism of the early stages of pathogenesis for

anthroponosis pneumonic plague induced by virulent *Y. pestis* F<sup>+</sup> strains is still unanswered.

One of properties of *Y. pestis* is the ability to form capsules.<sup>8</sup> Capsule synthesis is maximal at 37 °C in the absence of extracellular calcium.<sup>9</sup> The importance of capsular proteins in infectivity is exemplified by the F1 antigen. Capsular material (Caf1<sup>1</sup> or F1 antigen) is associated with both increased resistance to phagocytosis<sup>10</sup> and virulence.<sup>11</sup> Further, the absence of F1 antigen synthesis by *Y. pestis* leads to increased survival time of some infected host species.<sup>12</sup> Both active immunization with F1 from either a recombinant vector or *Y. pestis* and passive immunization with F1 monoclonal antibody protected mice from experimental infection.<sup>13</sup>

The F1 antigen is normally shed into the culture medium in polymeric form from either *Y. pestis*<sup>14</sup> or recombinant *E. coli*.<sup>15</sup> Brief heating at 100 °C of polymeric F1 antigen in buffered salt solutions at pH 4.4–7.5 followed by rapid cooling to 23 °C leads to depolymerization of the antigen into tetramers or a mixture of tetramers/dimers of Caf1 subunits, which slowly repolymerize at room temperature.<sup>14</sup> This process of F1 polymerization—depolymerization is highly reversible. After being heated at 100 °C in the presence of 7 M urea and cooled to room temperature, the protein exists as a Caf1 stable dimer. Heating the polymerized Caf1 at 100 °C in the presence of 0.1% SDS and cooling to 23 °C leads to the stable monomer. In accordance with these

\* To whom correspondence should be addressed at the University of California. Tel: 831-459-2915. Fax: 831-459-2935. E-mail: uversky@hydrogen.ucsc.edu.

<sup>†</sup> Institute of Immunological Engineering.

<sup>‡</sup> University of California.

<sup>§</sup> Stanford University.

<sup>||</sup> Russian Academy of Sciences.

(1) Abbreviations: FTIR, Fourier transform infrared spectroscopy; CD, circular dichroism; UV, ultraviolet; ANS, 8-anilino-1-naphthalene sulfonate; SAXS, small-angle X-ray scattering; DSC, differential scanning calorimetry; PAGE, polyacrylamide gel electrophoresis;  $R_g$ , Stokes radius;  $M$ , molecular mass; Caf1, capsular antigen F1; Caf1M, capsule antigen F1 mediator; LMW, low molecular weight; IL, interleukin; IL-1R interleukin-1 receptor; Yop, *Yersinia* outer proteins.

results, the dimer of Caf1 subunits is stabilized by hydrophobic interactions and may represent the minimal building block in the F1 capsule.<sup>14</sup>

Despite the importance of F1 for understanding the virulence of *Y. pestis* and development of new anti-plague vaccines, little is currently known about the conformational properties of this capsular adhesin. Here, we report the results from a systematic investigation of structural properties, conformational stability, and functional peculiarities of recombinant F1 adhesin expressed on the surface of *E. coli*. Our data may represent the basis for the elaboration of new anti-infectious drugs.

## Experimental Section

**Materials. Bacterial Strains, Plasmids, and Culture Conditions.** For all the experiments, *E. coli* HB101, DH5 $\alpha$ , or BL21-(DE3) and C600 carrying the appropriate plasmid were grown at 37 °C in LB broth containing ampicillin (50 mg/mL). The p12R plasmid<sup>16</sup> contained the main fragment of the *Y. pestis* *fl*-operon, encoding molecular periplasmic chaperone (Caf1M), usher-protein of outer membrane (Caf1A), capsular antigen (Caf1), and expressing capsule. The pFM1 plasmid<sup>17</sup> contained two genes, encoding Caf1 and Caf1M proteins under the control of *tac*-promoter. The plasmids pET-TGATG-hLI-1 $\alpha$  and pPR-TGATG-hLI-1 $\beta$ -tsr have been described previously.<sup>18</sup>

**Cell Cultures and Growth Conditions.** The TEC2.HS human thymic epithelial cell line and the U-937 macrophage cell line were supplied from the Institute of Immunology, Moscow. TEC2.HS cells and U-937 cells were cultured on full RPMI-1640 and DMEM media, respectively, as suspension lines.

**Methods. Purification of Caf1.** Recombinant *Y. pestis* capsular protein, Caf1, was isolated from *E. coli* HB101 cells and transformed by p12R plasmid. The protein was purified to homogeneity using TSK-Fractogel-HW-55 (F) column chromatography on a Pharmacia FPLC apparatus. After chromatography, SDS-PAGE showed only one protein with a molecular mass of 17 kDa. Caf1 was free of detectable endotoxin, as measured by the limulus polyphemus lysate assay (E-Toxate, Sigma). The specificity of recombinant Caf1 was verified by immunoblotting using anti-Caf1 monoclonal antibodies.

**Purification of Caf1–Caf1M Complexes.** The Caf1–Caf1M complex was isolated from *E. coli* DH5 $\alpha$  cells transformed by pFM1 plasmid. The cells were suspended in 1/100 volume of 20  $\mu$ M Tris–HCl buffer pH 8.0, containing 20% sucrose and incubated for 5 min at 20 °C, pelleted by centrifugation at 10000g for 20 min, suspended in a cold solution of 10 mM MgCl<sub>2</sub>, and incubated for 5 min in ice. After centrifugation, the supernatant (periplasmic cell fraction), containing Caf1–Caf1M complex, was diluted with 20 mM ammonium acetate, pH 7.4 to a total protein concentration of 0.2–0.3 mg/mL and fractionated with MonoQ FPLC. The Caf1–Caf1M complex was eluted with 120 mM NaCl.

**Purification of Human IL-1 $\alpha$  and IL-1 $\beta$ .** Human recombinant IL-1 $\alpha$  and IL-1 $\beta$  were produced by *E. coli* BL21(DE3) and *E. coli* C600, respectively, transformed by the plasmids pET-TGATG-hLI-1 $\alpha$  or pPR-TGATG-hLI-1 $\beta$ -tsr. Recombinant IL-1 $\alpha$  or IL-1 $\beta$  was purified by gel filtration, ion-exchange chromatography, and high-pressure liquid chromatography<sup>18,19</sup> to greater than 98%. The biological activities of purified proteins detected by murine thymocyte proliferative responses were  $1 \times 10^8$  U per 1 mg of the protein.

**Electrophoresis.** SDS–polyacrylamide gel electrophoresis (SDS–PAGE) was performed according to Laemmli.<sup>20</sup> Gel electrophoresis under nondenaturing conditions was carried

out using a Pharmacia system with 4/30 polyacrylamide gel. Caf1 protein or Caf1–Caf1M complex was dissolved in 0.09 M Tris–borate buffer pH 8.4 containing 0.93 g/L Na<sub>2</sub>EDTA (100  $\mu$ g in 25  $\mu$ L) and applied to the gel. The gel was stained with Coomassie Brilliant Blue R250 or subjected to immunoblotting. The molecular masses of Caf1 oligomers were determined using a Pharmacia HMW calibration kit: thyroglobulin (669 kDa), ferritin (440 kDa), catalase (232 kDa), lactate dehydrogenase (140 kDa), and albumin (67 kDa).

**Immunoblotting.** Immunoblot analysis of Caf1 or Caf1–Caf1M complex after electrophoresis under nondenaturing conditions was performed using standard procedures.

**Depolymerization of Caf1.** Depolymerized forms of Caf1 were obtained from the naturally polymerized Caf1 protein by a brief heating of the protein solution in 50 mM sodium phosphate buffer pH 7.5 (100 °C, 10 min) and rapid cooling to 25 °C.<sup>14</sup>

**Spectroscopic Measurements.** CD measurements were carried out using an AVIV-60DS spectropolarimeter equipped with a temperature-controlled cell holder. The cell path length was 1.0 and 10.0 mm for far- and near-UV CD measurements, respectively. The protein concentration was 0.6 mg/mL.

Intrinsic and ANS fluorescence was measured with a Perkin-Elmer MPF-4 instrument with excitation at either 269 or 296 nm (intrinsic) or 350 nm (ANS). Protein concentration was 0.1 mg/mL and ANS concentration 1.0  $\mu$ M. FTIR ATR spectra were collected on a Nicolet 800SX FTIR spectrophotometer equipped with an MCT detector as described previously.<sup>21</sup> Data analysis was performed with GRAMS-32 (Galactic Industries). Secondary structure content was determined from curve fitting to spectra deconvoluted using second derivatives and Fourier self-deconvolution to identify component band position.

**Hydrodynamic Analysis.** The molecular mass of the proteins was determined by equilibrium ultracentrifugation<sup>22,23</sup> or by gel-filtration.<sup>24–28</sup> Centrifugation measurements were performed on a MOM ultracentrifuge (Hungary) using interference optics. Sedimentation measurements were performed on model E ultracentrifuge (Beckman, USA) using Schleiaren optics and UV absorption. Sedimentation coefficients were estimated at a protein concentration of 0.5–10 mg/mL and extrapolated to zero concentration. Gel-filtration measurements were carried out on a Superdex-75 column using a Pharmacia FPLC apparatus. To determine molecular mass of the proteins under native conditions, a gel filtration column was calibrated using proteins from a standard molecular mass marker set.<sup>24–28</sup> Hydrodynamic dimensions (Stokes radius,  $R_s$ ) of proteins in different conformational states were also measured by size-exclusion chromatography,<sup>26–28</sup> using a set of globular proteins with known  $R_s$  for the column calibration.<sup>27</sup>

**Small-Angle X-ray Scattering (SAXS).** SAXS measurements were performed using Beam Line 4-2 at Stanford Synchrotron Radiation Laboratory as previously described.<sup>29</sup> Radii of gyration ( $R_g$ ) were calculated according to the Guinier approximation.<sup>30</sup>

**Differential Scanning Calorimetry (DSC).** DSC experiments were performed on a DASM-1A microcalorimeter with a cell volume of 1 mL or using a computerized DASM-4A microcalorimeter with a cell of 0.47 mL and a heating rate of 1.0 and 2.0 K/min. The protein concentrations were between 1.0 and 5.0 mg/mL. The Van't Hoff and calorimetric enthalpies of melting were calculated as described.<sup>31,32</sup>

**Equilibrium Unfolding Induced by Strong Denaturants.** Experiments on the GdmCl- or urea-induced equilibrium

unfolding of Caf1 were performed as follows. Small aliquots of a protein stock solution in 50 mM sodium phosphate pH 7.5 were added to the reaction mixture containing the desired concentrations of urea or GdmCl in the presence of 0.1 M acrylamide. Those mixtures were then incubated for 40 h at room temperature to reach the equilibrium before measuring. Unfolding was detected by a decrease in the intrinsic protein fluorescence due to the increased accessibility of the Caf1 tyrosines to the acrylamide.

**pH-Induced Structural Alterations of Caf1.** Experiments on pH-induced unfolding and refolding of Caf1 were performed in 50 mM Gly-HCl (pH range 2.0–3.6, buffer A) or 50 mM sodium citrate/citric acid (pH range 3.0–6.0, buffer B) buffer systems. Desired pH values were achieved using 0.1 M NaOH or HCl. The protein was dissolved and incubated for 24 h in A or B buffer for the unfolding or refolding experiments, respectively. Small aliquots of the concentrated protein stock solutions were added to appropriate buffer, and equilibrated for 40 h prior the measurements.

**Radiolabeling of Caf1 and IL-1.** Radiolabeling of Caf1 protein and IL-1 was carried out using the Iodogen technique.<sup>33</sup> A 50  $\mu$ L aliquot of iodogen (1,3,4,6-tetrachloro-3 $\alpha$ , $\alpha$ -diphenylglycouril, 0.04 mg/mL in dichloromethane) was dispersed in the bottom of a polypropylene iodination vial and evaporated to dryness at room temperature under nitrogen. Sodium phosphate buffer (0.05 M, 10  $\mu$ L, pH 7.4) was added to the iodination vial, followed by Na<sup>125</sup>I (1 mCi, 50  $\mu$ M, 10  $\mu$ L) and 10  $\mu$ g of Caf1 or rHuIL-1 $\beta$  in 0.05 M sodium phosphate buffer. The iodination was allowed to proceed for 10 min and terminated by adding 500  $\mu$ L of protein-free 0.05 M sodium phosphate. Labeled Caf1 and IL-1 were separated from free iodine by chromatography on a small Sephadex G-25 column. The radiolabeled Caf1 and IL-1 $\alpha$ , $\beta$  ran as single bands in SDS polyacrylamide gel electrophoresis. The activity of <sup>125</sup>I-labeled Caf1, IL-1 $\alpha$ , or IL-1 $\beta$  was 0.09, 0.1, and 0.1 mCi/ $\mu$ g protein, respectively. Although the radiolabeled IL-1 $\alpha$ , $\beta$  lost about 80% of its activity when assayed by murine thymocyte proliferative responses, they retained binding activity to rabbit anti-IL1 $\alpha$ , $\beta$  antibodies. The radiolabeled Caf1 retained binding activity to murine anti-Caf1 monoclonal antibodies.

**Binding Assay of <sup>125</sup>I-Labeled Caf1 and IL-1 to the Cells.** To study the interaction of Caf1 and IL-1, attached cells of TEC2.HS line and cells of U-937 line were cultured in six-well plates (Nunc) for 72 h. The cells were collected, washed three times with culture medium, and resuspended up to 10<sup>7</sup> cells per milliliter. Different doses of <sup>125</sup>I-labeled Caf, or <sup>125</sup>I-labeled IL-1 were added to 300  $\mu$ L of cells and incubated for 1 h at 4 °C. After the incubation, 50  $\mu$ L of the cell suspension mixture was layered on 250  $\mu$ L of dibutylphthalate-bis(2-ethylhexyl)-phthalate mixture and centrifuged for 2 min at 14000g. The radioactivity of the pellets was measured with 1275 MINI GAMMA apparatus (LKB, WALLAC). To determine nonspecific binding of <sup>125</sup>I-labeled Caf1 or <sup>125</sup>I-labeled IL-1, a 1000-fold surplus of unlabeled Caf1 and IL-1 was added along with the labeled protein. The results were expressed as the mean cpm (specific binding) from which nonspecific binding level was subtracted.

## Results

**Structural Properties of Caf1 Protein. Electrophoresis under Nondenaturing Conditions.** When purified recombinant Caf1 protein obtained from the culture medium of *E. coli* HB101/p12R cells was subjected to PAGE under nondenaturing

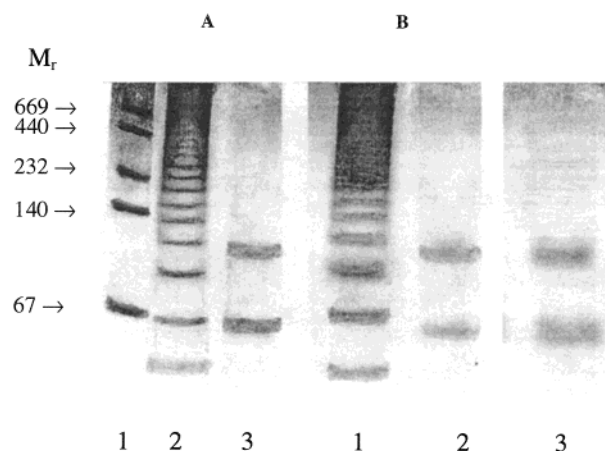


**Figure 1.** (A) Electrophoresis of *Y. pestis* Caf1 capsular protein and Caf1-Caf1M complex under nondenaturing conditions. Lanes: (1) protein markers; (2) Caf1 protein; (3) Caf1-Caf1M complex. (B) Immunoblot analysis of Caf1 and Caf1-Caf1M complex after electrophoresis under nondenaturing conditions. Lanes: (1) Caf1 protein detected with rabbit anti-Caf1 IgG; (2) Caf1-Caf1M complex detected with rabbit anti-Caf1 IgG; (3) Caf1-Caf1M complex detected with rabbit anti-Caf1M IgG.

conditions, only oligomers with even numbers of subunits were observed (Figure 1A). The smallest oligomer was the dimer, with a molecular mass of 31 kDa. The same result was obtained when native PAGE was electroblotted and developed with rabbit anti-Caf1 IgG (Figure 1B).

In contrast, native PAGE of periplasmic Caf1 preparations showed only two bands with apparent molecular masses of 60 and 120 kDa (see Figure 1). Furthermore, both of these bands were co-stained with anti-Caf1 and anti-Caf1M antibodies, reflecting the fact that they corresponded to Caf1-Caf1M complexes. The stoichiometry of these complexes was estimated from known molecular masses of Caf1 and Caf1M (15.5 and 29 kDa, respectively): the 60 kDa band was attributed to the complex of one Caf1 dimer with one Caf1M monomer, while the 120 kDa complex contained a Caf1 tetramer and two Caf1M monomers. Thus, Caf1 appears to form tight complexes with the periplasmic molecular chaperone Caf1M limited to the formation of Caf1 tetramers.

**Hydrodynamic Properties of Caf1.** The molecular mass,  $M_r$ , of Caf1 was determined at neutral and acid pH by ultracentrifugation and gel filtration. Ultracentrifugation experiments showed that independent of the pH and protein concentration Caf1 exists predominantly in oligomeric forms. The degree of polymerization is diminished by decreased protein concentration. At high protein concentration ( $\sim$ 5 mg/mL) Caf1 was relatively homogeneous and characterized by an average molecular mass of  $\sim$ 7000 kDa. At the same time, gel-filtration investigations show that even very strong dilution ( $<$ 0.001 mg/mL) does not lead to dissociation of dimers into monomers (see Table 1).

This conclusion was confirmed by the results of SAXS analysis of 1.0 mg/mL protein solution. The Guinier plot for naturally polymerized Caf1 had biphasic character (data not shown) reflecting the coexistence of at least two very different size species. The larger component consists of very large polymers, whereas the smallest component is characterized by an  $R_g$  value of 21.9 Å, which may correspond to the dimer.

Data presented in Table 1 allow some conclusions to be made about the shape of the Caf1 molecule. The relationship



**Table 1.** Hydrodynamic Properties and Apparent Molecular Masses Estimated for Naturally Polymerized *Y. pestis* Caf1 Capsular Protein by Analytical Ultracentrifugation, Nondenaturing Polyacrylamide Gel Electrophoresis, Gel Filtration, and SAXS

protein: condition	$M_r$ , kDa	$M_r^{\text{PAGE}}$ , kDa	$V_{\text{el}}$ , mL	$M_r^{\text{SEC}}$ , kDa	$R_s$ , Å	$R_g$ , Å	$R_s/R_g$
Caf1: pH 7.5	7000	31 <sup>a</sup>	14.21 <sup>b</sup>	31.3 <sup>b</sup>	25.4 <sup>b</sup>	21.9 <sup>c</sup>	1.16

<sup>a</sup> Values estimated for the smallest polymeric form of Caf1. <sup>b</sup> Values estimated at 0.001 mg/mL for the smallest polymeric form of Caf1. <sup>c</sup> Values estimated on the smallest polymeric form of Caf1.

between  $R_s$  and  $R_g$  is quite sensitive to the shape and compactness of the protein, for example,  $R_s/R_g = P^{1/3}[5/(P^2 + 2)]^{1/2}$ , where  $P = a/b$ , and  $a$  and  $b$  are the semiaxis of the revolution of the ellipsoid and the equatorial radius of the ellipsoid, respectively.<sup>34–36</sup> For an ideal spherical particle  $a = b$  and  $R_s/R_g = 1.29$ , whereas for globular proteins the average value of this relationship is about 1.25.<sup>37</sup> For many globular proteins, the shape is significantly nonspherical. In particular, the  $a/b$  ratio is  $\sim 2$  ( $R_s/R_g \sim 1.15$ ) for such “typical” globular proteins as ribonuclease,  $\alpha$ -chymotrypsin, pepsin,  $\beta$ -lactoglobulin, and chymotrypsinogen A.<sup>37</sup> Table 1 shows that this is also the case for the dimer of Caf1 ( $R_s/R_g = 1.16$ ). This means that the Caf1 dimer is a slightly asymmetrical particle with the  $a/b$  ratio of about 2.

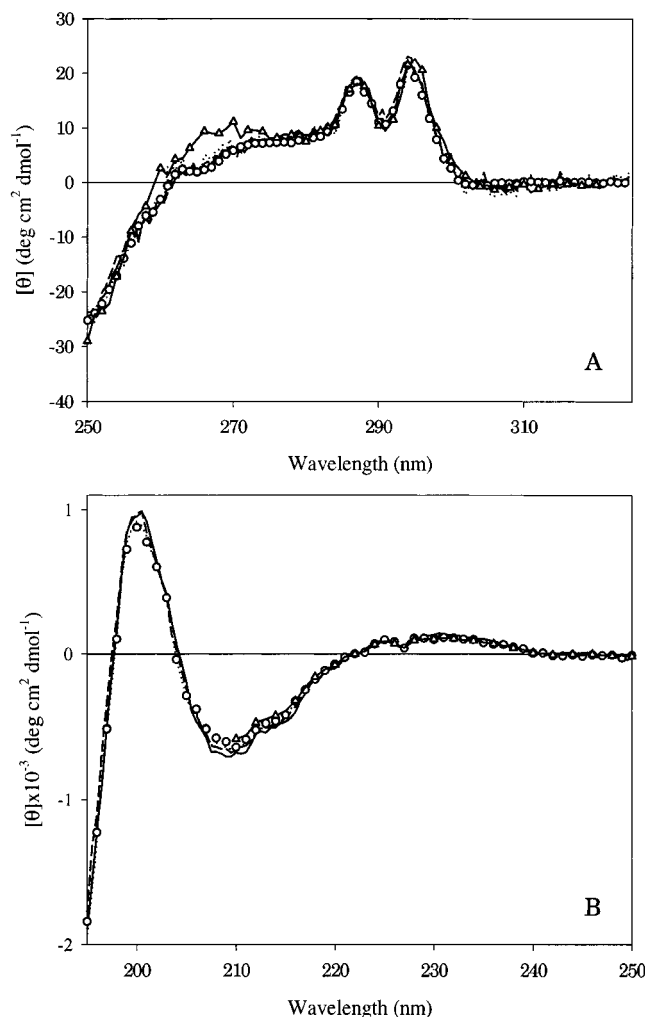
#### Near- and Far-UV CD Spectra of Different Caf1 Species.

Figure 2 represents near- and far-UV CD spectra of naturally polymerized capsule protein Caf1 of *Y. pestis* measured under various experimental conditions. The near-UV CD spectrum of this protein is characterized by the presence of two well-pronounced positive peaks in the vicinity of 287 and 294 nm (Figure 2A). As there are no tryptophan residues in Caf1, the presence of longer wavelength peaks in the near-UV CD spectrum suggests the existence of specific clusters of aromatic (Tyr, Phe) residues.

Figure 2B shows that the far-UV CD spectrum of naturally polymerized Caf1 is rather unusual (cf. ref 14). It is known that the shape of far-UV CD spectra can be considerably distorted due to the contribution of aromatic side chains.<sup>38–45</sup> Interestingly, such an effect is usually more pronounced for  $\beta$ -proteins, and the largest deviations from the “normal” spectrum have been reported for human carbonic anhydrase B,<sup>44–47</sup> and retinol binding protein.<sup>48</sup> The spectrum of naturally polymerized Caf1 resembles these unusual spectra.

Significantly, both the near- and far-UV CD spectra of naturally polymerized Caf1 were almost indistinguishable from those of the thermally depolymerized or stable dimeric form (shown in Figure 2 as circles and triangles, respectively). This means that the tertiary and secondary structure of the protein do not undergo any significant changes in the process of depolymerization, at least to the stage of dimers.

**Secondary Structure Analysis by FTIR.** Figure 3 represents the FTIR spectrum of naturally polymerized Caf1 (bold line) and the result of its deconvolution into component bands (thin lines). The details of the secondary structure analysis are given in Table 2. The high-frequency  $\beta$ -sheet band ( $1637\text{ cm}^{-1}$ ) makes the greatest contribution to the spectrum (43.5%). On the other hand, Table 2 shows that Caf1 contains 16.3% and 13.7%  $\alpha$ -helical and disordered structure, respectively (corresponding to bands with maxima at  $1662$  and  $1651\text{ cm}^{-1}$ , respectively). This means that naturally polymerized Caf1 should be classed



**Figure 2.** pH dependence of near (A) and far (B) UV CD spectra of *Y. pestis* Caf1 capsular protein. Measurements were carried out at 25 °C and pH 7.5 (solid line), pH 4.0 (dotted line), and pH 2.0 (dashed line). Circles and triangles show spectra of low molecular mass (obtained by brief heating of Caf1 for 10 min, at 100 °C in 50 mM sodium phosphate buffer, pH 7.5 and rapid cooling to 25 °C) and stable dimeric forms of Caf1 (obtained by brief incubation of the naturally polymerized protein at 100 °C in the presence of 7 M urea and cooling to 23 °C), respectively (ref 14). Protein concentration was 0.6 and 1.0 mg/mL, with cell path lengths 10 and 0.1 mm for near- and far-UV CD spectra measurements, respectively.

as a  $\beta$ -structural protein, which is in good agreement with the results of theoretical prediction.<sup>49</sup>

**ANS Fluorescence.** The ANS dye is frequently used for characterization of the degree of hydrophobicity of native proteins<sup>50</sup> and for the detection of non-native conformations in globular proteins.<sup>51</sup> ANS exhibits a considerable increase in fluorescence intensity and a pronounced blue shift of fluorescence maximum when it interacts with solvent-exposed hydrophobic clusters of protein. We have established that spectra of ANS in the presence of naturally polymerized Caf1, thermally depolymerized, or stable dimeric forms of Caf1 were almost indistinguishable from that of free ANS (data not shown). This means that all Caf1 forms studied do not have solvent exposed hydrophobic surfaces.

**Conformational Stability of Caf1. pH Stability.** Both near-UV (Figure 2A) and far-UV (Figure 2B) CD spectra of naturally

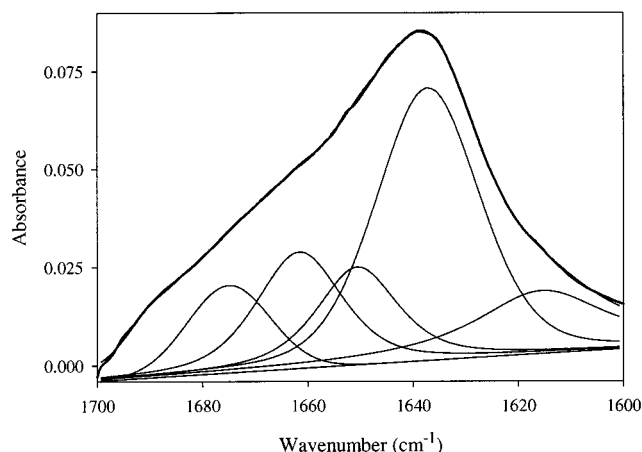


**Figure 3.** Secondary structure analysis of naturally polymerized *Y. pestis* Caf1 capsular protein by FTIR. FTIR spectrum of Caf1 is shown by a bold line, whereas its curve-fit spectrum is shown by thin line.

**Table 2.** Secondary Structure Content of Naturally Polymerized *Y. pestis* Capsule Protein Caf1 Determined by FTIR

structural assignment	wavenumber (cm <sup>-1</sup> )	% yield
turn	1689	3.7
turn	1675	10.3
$\alpha$ -helix/loop	1662	16.3
disordered	1651	13.7
$\beta$ -sheet	1637	43.5
$\beta$ -sheet	1616	12.5

polymerized Caf1 remain unchanged as the pH decreases from pH 7.5 to 2.0. This means that neither the tertiary nor secondary structure of this protein is affected by acidification of the solution. The data presented above are consistent with the suggestion that Caf1 belongs to the type III class of protein, which shows no significant structural changes at acidic pH.<sup>52</sup> This class includes such proteins as T4 lysozyme, chicken lysozyme, chymotrypsinogen, ubiquitin, concanavalin A, protein A, and  $\beta$ -lactoglobulin.<sup>52</sup>

**Stability toward Temperature-Induced Denaturation.** Thermal denaturation of naturally polymerized Caf1 (3–5 mg/mL, 150 mM NaCl, pH 7.5) monitored by DSC is characterized by an intense heat absorption in the vicinity of 364 K (91 °C) (Figure 4). Comparison of the calorimetric and effective enthalpies for Caf1 thermal denaturation shows that  $\Delta H^{\text{cal}}/\Delta H^{\text{eff}}$  is about 0.5, reflecting the fact that the cooperative unit of this process is a dimer of Caf1 subunits (see Figure 4).

**Stability toward Denaturant-Induced Unfolding.** The *Y. pestis* capsule protein Caf1 contains four tyrosines, Tyr23, Tyr51, Tyr71, and Tyr138, but no tryptophan residues. Unlike tryptophan fluorescence, the position of maximal emission of tyrosine is insensitive to the polarity of the environment. Nevertheless, the intensity of tyrosine fluorescence emission is extremely sensitive to the chromophore microenvironment.<sup>53</sup> Surprisingly, the intensity of Caf1 intrinsic fluorescence is unaffected by 8.4 M GdmCl (cf. curves 1 and 2, inset to Figure 5). This finding means that the local environment of the tyrosine residues remains unchanged even in the presence of high concentrations of strong denaturant.

To have more information about the environment of the tyrosines, we investigated the efficiency of their fluorescence quenching by the neutral quencher acrylamide.<sup>54,55</sup> The inset

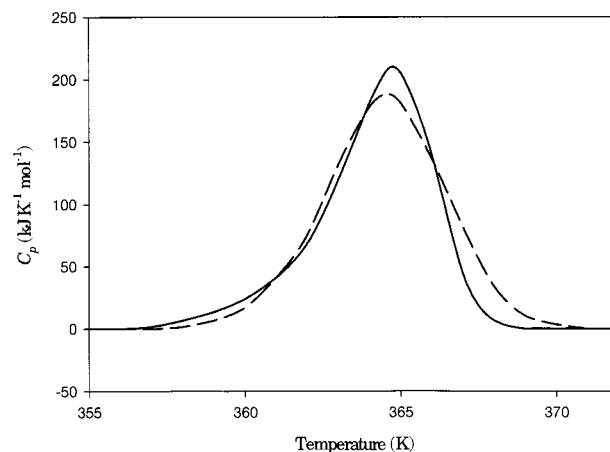


**Figure 4.** Thermal stability of naturally polymerized *Y. pestis* capsule protein Caf1 measured by scanning microcalorimetry. Panel represents experimental (solid line) and calculated (dashed line) curves of excess heat capacity. The latter was calculated assuming that the cooperative unit of the melting process is a dimer of Caf1 subunits. Measurements were carried out at pH 7.2, 150 mM NaCl, and a protein concentration of 3.5 mg/mL.

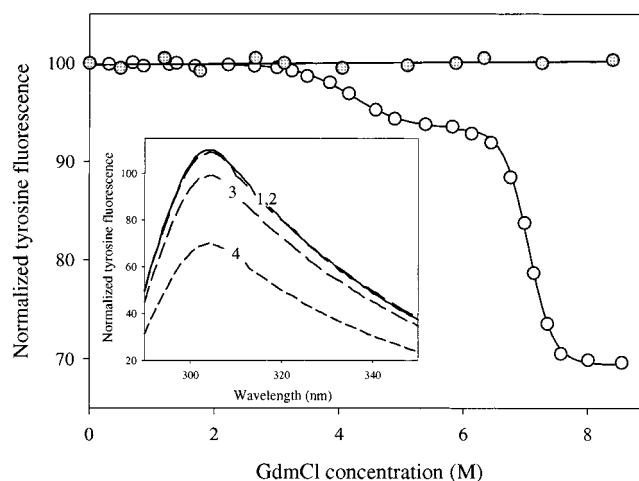


**Figure 5.** Effect of GdmCl on the structural properties of *Y. pestis* Caf1 capsular protein studied at different protein concentrations: 0.01 mg/mL Caf1 (open symbols) and 0.1 mg/mL Caf1 (gray symbols). Protein was dissolved in 50 mM sodium phosphate buffer, pH 7.5. Small aliquots of this stock solution were added to reaction mixtures containing the desired concentrations of GdmCl in the presence of 0.1 M acrylamide. These protein solutions were then incubated for 40 h at room temperature to reach equilibrium. Unfolding was detected as a characteristic decrease in the intrinsic fluorescence, due to the increased accessibility of the Caf1 tyrosines to the acrylamide quenching. The inset represents intrinsic fluorescence spectra measured for 0.05 mg/mL Caf1 in the absence (curves 1 and 3) or presence of 8.4 M GdmCl (curves 2 and 4). In the case of curves 3 and 4, the measurements were performed in the presence of 0.1 M acrylamide.

to Figure 5 shows that the addition of 0.1 M acrylamide to the unfolded protein solution (at a Caf1 concentration of 0.01 mg/mL) results in very effective quenching of the fluorescence (cf. curves 3 and 4). We used this observation for further characterization of Caf1 unfolding.

Figure 5 represents data on equilibrium GdmCl-induced unfolding of Caf1 protein monitored by changes in the intrinsic

fluorescence intensity in the presence of 0.1 M acrylamide. The unfolding of Caf1 in diluted solution is a complex process, with the unfolding curve consisting of two sequential transitions. The first of these transitions has  $C_m = 3.4$  M GdmCl and involves ~30% of the signal change. It may correspond to the dissociation of Caf1 oligomers. The second transition, with  $C_m = 7.0$  M GdmCl, may correspond to the complete unfolding of the protein. This means that even in very diluted solution Caf1 shows extremely high resistance toward the GdmCl-induced unfolding. Interestingly, in the same experiments with urea, we were unable to detect any decrease in the Caf1 intrinsic fluorescence even at 10.5 M urea.

Because purified Caf1 is an aggregated species, its stability may depend on concentration. We have studied Caf1 unfolding in a wide range of protein concentrations from 0.01 to 3.0 mg/mL. GdmCl unfolding experiments were performed using fluorescence at two protein concentrations, 0.01 and 0.1 mg/mL. Figure 5 shows that GdmCl induces structural changes in very dilute Caf1 solutions (0.01 mg/mL), whereas in more concentrated solutions (0.1 mg/mL) the protein structure is absolutely unaffected by 8.4 M GdmCl (cf. open and gray symbols). This conclusion was confirmed by SAXS and CD experiments. SAXS profiles measured for 3.0 mg/mL Caf1 solutions remained unchanged in a wide range of denaturant concentrations (from 0 to 10.5 M urea or to 8.4 M GdmCl, data not shown), while near-UV CD measurements at 1.0 mg/mL Caf1 in the presence of high concentrations of these denaturants also did not reveal any changes in spectral shape or intensity (data not shown). This means that the naturally polymerized Caf1 possesses extremely high stability toward strong denaturants and this stability depends on the protein concentration.

**Functional Analysis of *Y. pestis* Capsular Antigen Caf1. Binding of Caf1 with Human Macrophages of U-937 Cell Line and Thymic TEC2.HS Cells.** Previously, the specific binding of  $^{125}$ I-labeled Caf1 to IL-1R murine fibroblasts from NIH 3T3 cells has been detected.<sup>56</sup> Further, it was demonstrated that the Caf1–Caf1M complex effectively inhibited IL-1 $\beta$  binding to *E. coli* HB101/p12R cells expressing the IL-1 receptor (IL-1R), while no inhibition of huIL-1 $\beta$  binding by free Caf1M was observed.<sup>17</sup> The lack of specific inhibition of IL-1 $\beta$  binding by naturally polymerized Caf1, purified from the culture medium of recombinant *E. coli*, was also established. Our results are consistent with Caf1M chaperone limiting the oligomerization of Caf1 protein to tetramers. Thus, only low molecular weight (LMW) oligomers of Caf1 may interact efficiently with IL-1R.

Knowing this, we performed the binding experiments with tetrameric/LMW fractions of Caf1. For this purpose the naturally polymerized protein was depolymerized by a brief heating of the protein solution in 50 mM sodium phosphate buffer, pH 7.5 (100 °C, 10 min) and rapid cooling to 25 °C.<sup>14</sup>

In our study, human thymic epithelial cells (TEC2.HS) and macrophage (U-937) cell lines have been used for the analysis of Caf1 binding to IL-1R. The presence of IL-1R on the cell surface of TEC2.HS and U-937 cell lines was supported by experiments to detect binding to  $^{125}$ I-labeled IL-1 $\alpha$  and  $^{125}$ I-labeled IL-1 $\beta$ , respectively. Specific interaction of  $^{125}$ I-labeled IL-1 $\beta$  with IL-1R of U-937 cells was characterized by  $K_d = (0.5 \pm 0.02) \times 10^{-10}$  M (Figure 6), while  $^{125}$ I-labeled IL-1 $\alpha$  bound to TEC2.HS cells with  $K_d = (3.9 \pm 0.1) \times 10^{-10}$  M (Figure 7). Similarly, the binding of  $^{125}$ I-labeled Caf1 to IL-1R of U-937 cells was characterized by  $K_d = (0.8 \pm 0.02) \times 10^{-10}$  M (Figure 6) and to TEC2.HS cells with a  $K_d = (1.8 \pm 0.2) \times 10^{-9}$  M (Figure

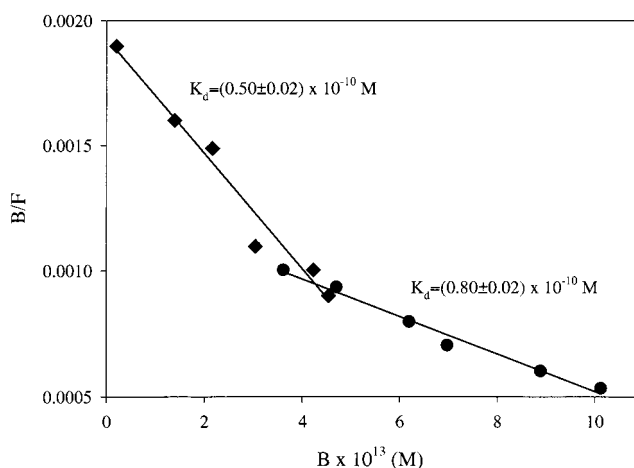


**Figure 6.** Scatchard analysis for the specific binding of Caf1 (●) and IL-1 $\beta$  (◆) to human macrophage cells of U937 cell line. Because of the heterogeneity of Caf1 oligomer composition, the calculations were made assuming a molar mass of tetramer. This assumption follows from the fact that the tetramer was shown to be the predominate oligomer in preparations of capsular protein heated to 100 °C and stored 4–6 h (ref 14).

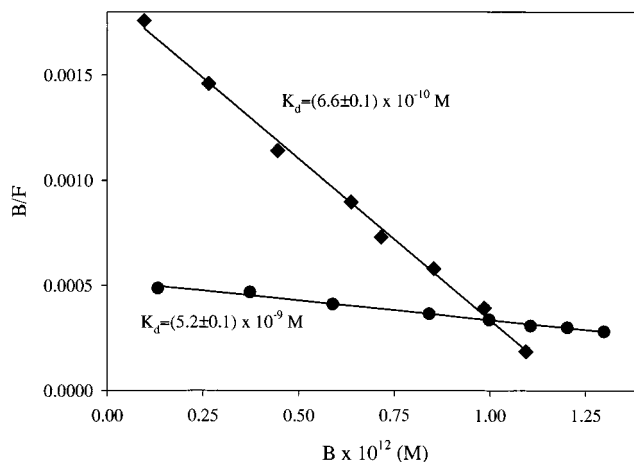


**Figure 7.** Scatchard analysis for specific binding of Caf1 (●) and IL-1 $\alpha$  (◆) to attached human thymic epithelial cells of TEC2.HS cell line. Because of the heterogeneity of Caf1 oligomer composition, the calculations were made assuming a molar mass of tetramer. This assumption follows from the fact that the tetramer was shown to be the predominate oligomer in preparations of capsular protein heated to 100 °C and stored 4–6 h (ref 14).

7). The specificity of such interactions was confirmed by the inhibition of IL-1 $\alpha$  binding by Caf1 (see Figure 8).

## Discussion

**Caf1 as *Y. pestis* Adhesin.** We have shown that a Caf1 dimer is the minimal cooperative block of the natural Caf1 polymer. Moreover, we have established that Caf1 binds specifically to the IL-1R on the surfaces of human thymic epithelial cells (TEC2.HS line) and macrophagal cells (U-937 line) only when depolymerized to the dimeric or LMW form. The specificity of such interaction was confirmed by the inhibition of IL-1 $\alpha$  binding by Caf1.

*Y. pestis* virulence correlates with the stability of this bacteria to phagocyte uptake and with its ability to survive and proliferate in phagocytic cells.<sup>57,58</sup> While alveolar macrophages

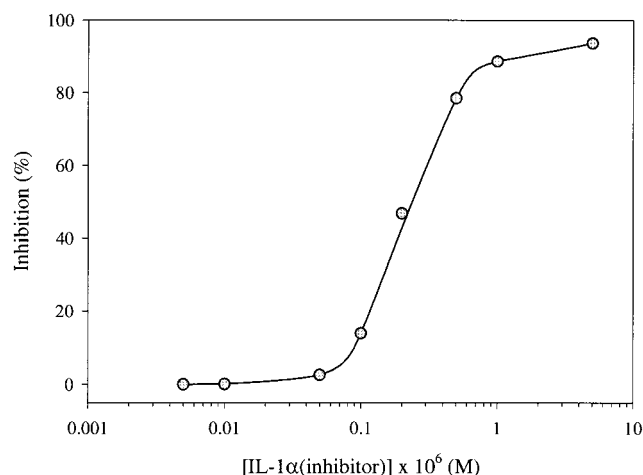


**Figure 8.** Inhibition of specific binding of  $^{125}\text{I}$ -Caf1 and IL-1 $\alpha$  to attached human thymic epithelial cell of TEC2.HS cell line.

represent the most important part of the cellular mechanism of lung defense against inhaled particles,<sup>59</sup> the plague agent had both the ability to resist the main bactericidal oxygen-dependent mechanisms of phagocytes and the ability to damage macrophages on contact with them via formation of a transmembrane channel and following injection through the eukaryotic cell membrane of effector Yop-proteins (*Yersinia* outer proteins), paralyzing macrophage function.

It is known that special surface adhesion structures are responsible for the contact of pathogenic Gram-negative bacteria with the host cell. Polarized translocation of Yop-proteins inside the phagocyte and realization of the Yop-virulon system occurs only at the site determined by the interaction of bacterial adhesin with the host receptor under conditions of tight contact between the pathogen and the host cell.<sup>60–62</sup> The proteins Inv, YadA, and Ail perform the adhesion function in the human pathogens *Yersinia pseudotuberculosis* and *Yersinia enterocolitica*.<sup>63</sup> However, unlike *Y. pseudotuberculosis* and *Y. enterocolitica*, the situation with respect to the existence of such specialized adhesion structure for *Y. pestis* is still not clear, although all three bacteria have a homologous “virulence” plasmid (pYV or pIB, pCD, pCad, Lcr-plasmid).<sup>64–67</sup> In this regard, the ability of Caf1 to interact with IL-1R of immunocompetent cells could be evidence of the adhesive function of capsule subunits responsible for bacterial contact with the host cells and, as consequence, for formation of the initiation signal for *Y. pestis* Yop-virulon proteins expression and secretion.<sup>67</sup> Moreover, the competition between Caf1 and IL-1 for IL-1R observed in our study may be crucial for the realization of the Caf1 adhesive function. In this way, the tight binding of Caf1 to IL-1R could represent the primary step in the *Y. pestis* pathogenicity, keeping the bacteria on the macrophage or lung epithelial cell surface. In turn, this initiates the type III secretion system, specialized in the secretion of the virulence factors into the host cell. Finally, the formation of all studied specialized surface adhesion structures is regulated by periplasmic molecular chaperones.<sup>68,69</sup> It should be noted that periplasmic chaperones are also involved in the biogenesis of *Y. pestis* capsule, which may underline the exceptional significance of the adhesion structures for the virulence manifestation by this pathogenic bacterium.

The ability of *Y. pestis* bacteria to form a protective capsule consisting of the polymeric form of Caf1 was established more than 100 years ago.<sup>7</sup> Caf1 protein was shown to aggregate into

a large gel-like capsule or envelope at 37 °C, whereas, if cultured at 28 °C, *Y. pestis* does not form such a capsule. However, even under these conditions a minimal quantity of Caf1 was detected serologically on the bacterial cell surfaces.<sup>70</sup> Interestingly, the plague bacteria in this case were as virulent as those grown at 37 °C apparently having functional capsules.

We assume that the ability of LMW Caf1 to interact with IL-1 receptors of several immunocompetent cells may be responsible for the formation of a tight contact between *Y. pestis* and the target cell by a Caf1 dimer bound to the Caf1A usher protein of *Y. pestis* outer membrane. According to this model, plague bacteria have to contain on their surfaces dimeric or/and LMW oligomeric forms of Caf1 to manifest adhesive function and to form a tight contact with the host-cell and initiation of the type III secretion system.

**Possible Role of Caf1 Capsular Antigen in the Primary Pneumonic Plague Development.** Obviously, such an adhesive function could be realized easily during the initiation of the bubonic plague. It is well-known that the transmission of plague between rodents is accomplished by their associated fleas, which acquire *Y. pestis* from an infected blood meal.<sup>4</sup> As the reproduction of *Y. pestis* in a flea occurs at a temperature lower than 37 °C, bacteria penetrating into the host organism because of a flea bite will have Caf1 in dimeric or/and LMW oligomeric forms on their surfaces. Thus, flea-regurgitated bacteria are capable of realizing the adhesive activity and the subsequent expression of genes of the Yop-virulon.

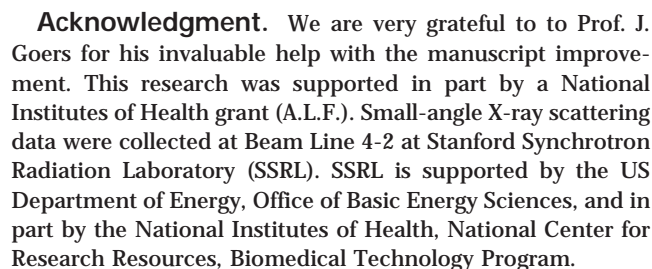
The situation with regard to the involvement of Caf1 as an adhesin in the development of primary pneumonic plague is more complex. This is because bacteria have to lose their capsules (high molecular oligomeric forms of Caf1), keeping Caf1 in dimeric or/and LMW oligomeric forms on their surfaces, to achieve adhesive function. We assume that depolymerization could occur as a result of partial denaturation of capsular Caf1 protein on the surface of water–air interfaces. A possible scenario is considered below.

Initially, plague bacteria covered by high molecular weight polymer capsule is released within an aerosol spread by a patient with pneumonic plague while sneezing, coughing, or talking. The capsule may protect the plague bacteria from environment in large droplets for a certain period of time. It is known that proteins are readily adsorbed at the air–water interface,<sup>71–74</sup> where they may undergo major structural transformations.<sup>73–79</sup> This means that plague bacteria in small aerosol droplets suspended in the air may lose the capsule naturally under the influence of forces originating on the surface of the liquid/air interface. The loss of the capsule will lead to formation of Caf1 dimers, the minimal cooperative and structural unit.

Following inhalation into the lung the aerosol droplet containing *Y. pestis* cells with shed and depolymerized capsule may contact the lung surfactant system and dissolve in alveolar fluid. This rapid dilution of Caf1 dimers could exclude the possibility of capsule repolymerization and restoration on bacterial cell. As a result, bacteria may contain dimeric or/and LMW oligomeric forms of Caf1 anchored by Caf1A, which are ready to interact with IL-1R as adhesins (see Figure 9).

Depolymerization of the Caf1 capsule may have several other pathological implications. We have recently shown that following depolymerization by heating, Caf1 is able to bind effectively to IL-1 $\beta$ .<sup>56</sup> In fact, binding of free Caf1 dimers to IL-1 $\beta$  may restrict cytokines ability to bind type I receptors, thus blocking the interleukin function as a key mediator of immune





- (46) Jagannadham, M. V.; Balasubramanian, D. *FEBS Lett.* **1985**, *188*, 326–330.
- (47) Rodionova, N. A.; Semisotnov, G. V.; Klityshenko, V. P.; Uversky, V. N.; Bolotina, I. A.; Bychkova, V. E.; Ptitsyn, O. B. *Mol. Biol. (Moscow)* **1989**, *23*, 683–692.
- (48) Bychkova, V. E.; Berni, R.; Rosi, J. L.; Kutysheko, V. P.; Ptitsyn, O. B. *Biochemistry* **1992**, *31*, 7566–7571.
- (49) Galyov, E. E.; Smirnov, O. Yu.; Karlyshev, A. V.; Volkovoy, K. I.; Denesyuk, A. I.; Nazimov, I. V.; Rubtsov, K. S.; Abramov, V. M.; Dalvadyanz, S. M.; Zav'yalov, V. P. *FEBS Lett.* **1990**, *277*, 230–232.
- (50) Stryer, L. *J. Mol. Biol.* **1965**, *13*, 482–485.
- (51) Semisotnov, G. V.; Rodionova, N. A.; Razgulyaev, O. I.; Uversky, V. N.; Gripas, A. F.; Gilmanshin, R. I. *Biopolymers* **1991**, *31*, 119–128.
- (52) Fink, A. L.; Calciano, L. J.; Goto, Y.; Kurotsu, T.; Palleros, D. R. *Biochemistry* **1994**, *33*, 12504–12511.
- (53) Schmid, F. X. In *Protein Structure. A Practical Approach*; Creighton, T. E.; Ed.; IRL Press at Oxford University Press: Oxford, 1997; pp 261–297.
- (54) Eftink, M. R.; Ghiron, C. A. *Anal. Biochem.* **1981**, *114*, 199–227.
- (55) Uversky, V. N. *Biochemistry (Moscow)* **1999**, *64*, 250–266.
- (56) Abramov, V. M.; Vasiliev, A. M.; Vasilenko, R. N.; Kulikova, N. L.; Kosarev, I. V.; Khlebnikov, V. S.; Ishchenko, A. T.; MacIntire, S.; Khurana, R.; Gillespie, J. R.; Fink, A. L.; Uversky V. N. *Biochemistry* **2001**, *40*, 6076–6084.
- (57) Cavanaugh, D. C.; Randall, R. *J. Immunol.* **1959**, *83*, 348–371.
- (58) Burrows, T. W. *Ergeb. Mikrobiol. Immun. Exp. Ther.* **1963**, *37*, 59–113.
- (59) Fedoseev, G. B.; Lavrova, T. V.; Zykcharev, S. S. *Cellular and Subcellular Mechanisms for Defense and Damage of Bronchi and Lungs*; Nauka: Leningrad, 1980; 198pp.
- (60) Cornelis, G. R.; Wolf-Watz, H. *Mol. Microbiol.* **1997**, *23*, 861–867.
- (61) Cornelis, G. R. *Bacteriol.* **1998**, *180*, 5495–5504.
- (62) Galan, J. E.; Collmer, A. *Science* **1999**, *284*, 1322–1328.
- (63) Miller, V. L. *Trends Microbiol.* **1995**, *3*, 654–658.
- (64) Feber, D. M.; Brubaker, R. R. *Infect. Immun.* **1981**, *31*, 839–841.
- (65) Portnoy, D. A.; Moseley, S. L.; Falkow, S. *Infect Immun.* **1981**, *31*, 775–782.
- (66) Portnoy, D. A.; Falkow, S. *J. Bacteriol.* **1981**, *148*, 877–883.
- (67) Portnoy, D. A.; Wolf-Watz, H.; Bolin, I.; Beeder, A. B.; Falkow, S. *Infect Immun.* **1984**, *43*, 108–114.
- (68) Hultgren, S. J.; Abraham, S.; Caparon, M.; Falk, P.; St. Geme, J. W., III; Normark, S. *Cell* **1993**, *73*, 887–901.
- (69) Jacob-Dubuisson, F.; Kuehn, M.; Hultgren, S. J. *Trends Microbiol.* **1993**, *1*, 50–55.
- (70) Bicchul, O. K.; Lebedeva, S. A.; Alekseeva, L. P. *Microbiol. Lab. Diagnost. (Saratov)* **1989**, 44–49.
- (71) Zakrevskiy, V. I.; Plekhanova, N. G. *Vestn. Akad. Med. Nauk SSSR* **1990**, *8*, 41–44.
- (72) Graham, D. E.; Phillips, M. C. *J. Colloid Interface Sci.* **1979**, *70*, 403–414.
- (73) Tripp, B. C.; Magda, J. J.; Andrade, J. D. *J. Colloid Interface Sci.* **1995**, *173*, 16–27.
- (74) Xu, S. Q.; Damodaran, S. *J. Colloid Interface Sci.* **1993**, *159*, 124–133.
- (75) Damodaran, S.; Song, K. B. *ACS Symp. Ser.* **1991**, *454*, 104–121.
- (76) Clarkson, J. R.; Cui, Z. F.; Darton, R. C.; Clarkson, J. R. *J. Colloid Interface Sci.* **1999**, *215*, 323–332.
- (77) Clarkson, J. R.; Cui, Z. F.; Darton, R. C. *J. Colloid Interface Sci.* **1999**, *215*, 333–338.
- (78) Colombie, S.; Gaunand, A.; Rinaudo, M.; Lindet, B. *Biotechnol. Lett.* **2000**, *22*, 277–283.
- (79) Maa, Y. F.; Hsu, C. C. *Biotechnol. Bioengng* **1997**, *54*, 506–512.

PR025511U